Proceedings of the 1996 IEEE
International Conference on Robotics and Automation
Minneapolis, Minnesota - April 1996

Pose from Pushing*

Yan-Bin Jia Michael Erdmann
The Robotics Institute
School of Computer Science
Carnegie Mellon University
Pittsburgh, PA 15213-3890

Abstract

In the absence of vision, grasping an object often relies on tactile feedback from the fingertips. Before force closure is formed, where on the object a fingertip touches can usually be felt from the motion of contact on the fingertip during a small amount of pushing. In this paper we investigate the first stage of such "blind" grasping. More specifically, we study the problem of determining the pose of a known planar object by pushing. *Assuming sliding friction in the plane, a dynamic analysis of pushing results in a numerical algorithm that computes the object pose from* three *instantaneous contact positions on a fingertip. Simulations and experiments (with an Adept robot) have been conducted to demonstrate the sensing feasibility.*

Inspired by the way a human hand grasps, this work can be viewed as a primitive step in exploring interactive sensing in grasping tasks.

1 Introduction

Part sensing and grasping are two fundamental operations in automated assembly. Traditionally, they are performed sequentially in an assembly task. Parts in many assembly applications are manufactured to high precisions based on their geometric models; so their shapes are known. The knowledge of part geometry can sometimes significantly facilitate sensing as well as grasping. It may also help integrate these two operations, reducing the assembly time and cost.

Consider the task of grasping something, say, a pen, on the table while your eyes are closed. Your fingers fumble on the table until one of them touches the pen and (inevitably) starts pushing it for a short distance. However, at this moment you can almost already tell which part of the pen is being touched by feeling how the contact is moving on the fingertip. Assume the pushing finger is moving away from you. If the contact remains almost stable, then the middle of the pen is being touched; if the contact moves counterclockwise on the fingertip, then the right end of the pen is being touched; otherwise the left end is being touched. Immediately, a picture of the pen configuration has been formed in your head so your other fingers quickly close in for a good grip.

The above example tells us that the pose of a known shape can sometimes be inferred from the contact motion on a finger pushing the shape. Figure 1 shows two motions of a quadrilateral in different initial poses pushed by a finger in the same motion. Although the initial contacts on the finger were the same, the final contacts are quite different. Thinking in reverse leads to the main question of this paper: *Can we determine the initial pose of an object from the contact motion on a pushing finger, or simply, from a few intermediate contact positions during the pushing?*

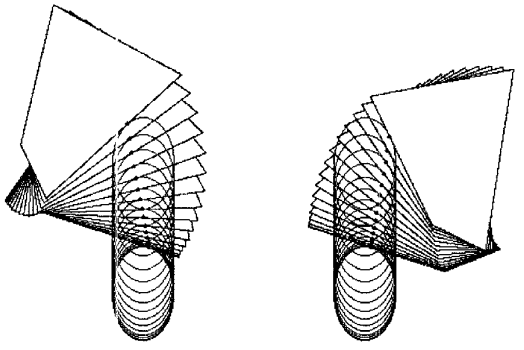

Figure 1: Different motions of contact (shown with dots) on an elliptic finger that result from pushing a quadrilateral in two different initial poses.

We give an affirmative answer to the above question in the general case. Section 2 studies the dynamics of pushing, deriving a set of differential equations that govern the con-

*Support for this research was provided in part by Carnegie Mellon University, and in part by the National Science Foundation through the following grants: NSF Presidential Young Investigator award IRI-9157643 and NSF Grant IRI-9213993.

tact motion and showing how to solve them numerically; Section 3 describes a numerical routine that computes the initial pose of an object from finite intermediate contact positions on a pushing finger; Section 4 presents simulations and experiments, which demonstrate that *three* intermediate contact points often suffice to determine the initial pose for the fingers and objects tested; Finally, Section 5 summarizes the paper and outlines the future work.

1.1 Previous Work

Mason [13] explores the mechanics of pushing using quasi-static analysis, predicting the direction in which an object being pushed rotates and plotting out its instantaneous rotation center. For unknown center of friction, Alexander and Maddocks [2] reduce the problem of determining the motion of a slider under some applied force to the case of a bipod and offer analytical solutions for simple sliders.

The work by Lynch *et al.* [11] localizes an object using the mechanics of pushing and tactile feedback; a control system has been developed to translate and orient objects. Akella and Mason [1] describe a complete open-loop planner that can orient and translate objects in the plane by pushing with a straight fence. Donald *et al.* [4] study the information structure of cooperative pushing tasks to reorient large objects, showing the equivalences between different types of sensing and communication by sensor reduction.

Dynamics of sliding rigid bodies is treated in MacMillan [12] for non-uniform pressure distributions, and in Goyal *et al.* [6] using geometric methods based on the limit surface description of friction. Assuming uniform pressure distribution and frictionless pushing contact, Section 2.3 presents a dynamic analysis that determines the initial acceleration and angular acceleration of an object given the pusher acceleration.

The problem of predicting the accelerations of multiple 3D objects in contact with Coulomb friction has a nonlinear complementarity formulation [15]; the existence of solutions to models with sliding and rolling contacts has been established.

In [14], Montana derives a set of differential equations describing the motion of a contact point in response to a relative motion of the objects in contact, and employs these equations to sense the local curvature of an unknown object or to follow its surface. The kinematics of spatial motion with point contact is also studied by Cai and Roth [3] who assume a tactile sensor able to measure the relative motion at the contact point. The special kinematics of two rigid bodies rolling on each other is considered by Li and Canny [10] in view of path planning in the contact configuration space.

In their review of robotic touch sensing [7], Howe and Cutkosky argue that shape and force are the most important quantities measured with touch sensors. The uses of touch information in object recognition and manipulation are classified and various sensing devices are discussed and compared.

Finally, the work presented here is closely related to our previous work [8] on sensing known shapes. Whereas in the previous work poses are derived from geometric constraints alone, here they are derived under manipulation operations from geometric constraints as well as kinematic and dynamic equations.

2 Motion of Contact

Consider the problem of a translating finger f pushing an object B in the plane. The coefficient of friction between B and the plane is everywhere μ. For simplicity, let us assume *frictionless* contact between f and B, and uniform mass (and thus pressure) distribution of B.

Let f's boundary be a twice differentiable curve α and B's boundary be a piecewise twice differentiable closed curve β such that $\alpha(u)$ and $\beta(s)$ locate the contact point on these two curves (in their local frames) respectively. Following convention, moving counterclockwise along α and β increases u and s. To avoid any ambiguity, the notation "$\dot{}$" means differentiation with respect to time, and the notation "$'$" means differentiation with respect to some curve parameter. For example, $\dot{\alpha} = \alpha' \dot{u} = \frac{d\alpha}{du}\frac{du}{dt}$ gives the velocity of the contact point on α. Assume that one curve segment on β stays in contact with α throughout the pushing. Let v_f be the velocity of f, v and ω the velocity and angular velocity of B respectively, all in the world coordinate frame (Figure 2).

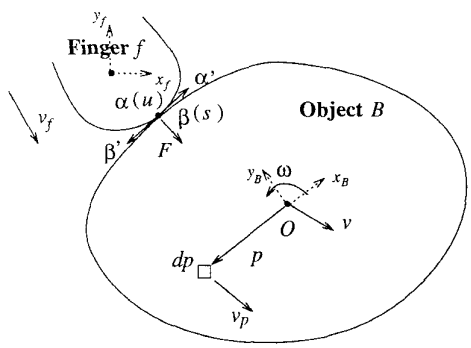

Figure 2: Pushing object B by finger f translating at velocity v_f.

That f and B maintain contact imposes a velocity constraint

$$v_f + \alpha' \dot{u} = v + \omega \times R\beta + R\beta' \dot{s}, \qquad (1)$$

where $R(\theta) = \begin{pmatrix} \cos\theta & -\sin\theta \\ \sin\theta & \cos\theta \end{pmatrix}$ is the rotation matrix associated with the orientation θ of B. Newton and Euler's

equations on rigid body dynamics are stated as

$$F + \int_B -\mu\rho g\hat{v}_p \, dp = ma, \quad (2)$$

$$R\beta \times F + \int_B Rp \times (-\mu\rho g\hat{v}_p) dp = I\dot{\omega}, \quad (3)$$

where F is the contact force acting on B, ρ the mass density (not necessarily uniform), g the gravitational acceleration, m the mass, a the acceleration of the center of mass O, and I the angular inertia about O (all of B). Here $v_p = v + \omega \times Rp$ is the velocity at $p \in B$ and $\hat{v}_p = \frac{v_p}{|v_p|}$ is its direction.[1]

With no friction at the contact point, F acts along the inward normal of B:

$$F \cdot R\beta' = 0; \quad (4)$$

$$R\beta' \times F > 0. \quad (5)$$

Finally, the normals of f and B at the contact are opposite to each other; equivalently, we have

$$\alpha' \times R\beta' = 0, \quad (6)$$

as $\alpha' \cdot R\beta' < 0$ always holds.

If the motion v_f of the finger is known, there are seven equations (1), (2), (3), (4), and (6) with seven unknowns u, s, v, ω, and F.[2] From these equations, we are now ready to derive the differential equations for u, s, v, and ω.

Taking the dot products of α' with both sides of (1) and rearranging terms thereafter, we obtain

$$|\alpha'|^2\dot{u} - (\alpha' \cdot R\beta')\dot{s} = \alpha' \cdot (v + \omega \times R\beta - v_f).$$

Next differentiate both sides of (6):

$$(\alpha'' \times R\beta')\dot{u} + (\alpha' \times R\beta'')\dot{s} + (\alpha' \cdot R\beta')\omega = 0.$$

Immediately, we can solve for $\dot{s}$ and $\dot{u}$ from the two equations above:

$$\dot{s} = -\Big((\alpha' \cdot R\beta')\omega|\alpha'|^2 + (\alpha'' \times R\beta')\big(\alpha' \cdot (v + \omega \times R\beta - v_f)\big)\Big) \Big/ \Big((\alpha' \cdot R\beta')(\alpha'' \times R\beta') + |\alpha'|^2\alpha' \times R\beta''\Big); \quad (7)$$

$$\dot{u} = \frac{\alpha' \cdot (v + \omega \times R\beta + R\beta'\dot{s} - v_f)}{|\alpha'|^2}. \quad (8)$$

[1] That f is translating implies either $v \neq 0$ or $\omega \neq 0$ after the pushing starts. So v_p can vanish over at most one point $p \in B$, which will vanish in the integrations in equations (2) and (3).

[2] Note that equations (1) and (2) and variables v and F are each counted twice.

If α and β are unit-speed curves with curvatures κ_α and κ_β, respectively, equations (7) and (8) are simplified to

$$\dot{s} = \frac{-\omega + \kappa_\alpha\alpha' \cdot (v + \omega \times R\beta - v_f)}{\kappa_\alpha + \kappa_\beta};$$

$$\dot{u} = \frac{\omega + \kappa_\beta\alpha' \cdot (v + \omega \times R\beta - v_f)}{\kappa_\alpha + \kappa_\beta}.$$

Now we move on to derive the differential equations for v and ω. First we take the cross products of $R\beta'$ with both sides of (3), eliminating the term containing $F \cdot R\beta'$ and substituting (2) in after term expansion:

$$-(\beta' \cdot \beta)ma - \mu\rho g\Gamma = R\beta' \times I\dot{\omega}.$$

Here the term

$$\Gamma = \int_B (R\beta' \cdot \hat{v}_p)Rp + \Big(\beta' \cdot (\beta - p)\Big)\hat{v}_p \, dp, \quad (9)$$

when multiplied by $\mu\rho g$, combines the dynamic effects of friction. Therefore

$$a = \frac{\mathcal{A}\eta^2\dot{\omega} \times R\beta' - \mu g\Gamma}{\mathcal{A}\beta' \cdot \beta}, \quad (10)$$

where $\mathcal{A} = \int_B dp = \frac{m}{\rho}$ and $\eta = \sqrt{\frac{I}{m}}$ are the area and the radius of gyration of B, respectively.

Taking the cross products of α' with both sides of (1) and cancelling the term $\alpha' \times R\beta'$ according to (6), we have after a few more steps of term manipulation

$$\alpha' \times (v_f - v) = (\alpha' \cdot R\beta)\omega. \quad (11)$$

Differentiating both sides of (11) yields

$$\alpha' \times a + (\alpha' \cdot R\beta)\dot{\omega} = \alpha''\dot{u} \times (v_f - v) + \alpha' \times a_f - \Big(\alpha''\dot{u} \cdot R\beta + \alpha' \cdot (\omega \times R\beta + R\beta'\dot{s})\Big)\omega. \quad (12)$$

Finally, substituting (10) in (12) gives:

$$\dot{\omega} = \Big(\alpha''\dot{u} \times (v_f - v) + \alpha' \times a_f - \Big(\alpha''\dot{u} \cdot R\beta + \alpha' \cdot (\omega \times R\beta + R\beta'\dot{s})\Big)\omega + \frac{\mu g}{\mathcal{A}\beta' \cdot \beta}\alpha' \times \Gamma\Big) \Big/ \Big(\alpha' \cdot R\Big(\beta + \frac{\eta^2}{\beta' \cdot \beta}\beta'\Big)\Big). \quad (13)$$

Equations (7), (8), (10), (13), and $\dot{\theta} = \omega$ form a system of ordinary differential equations that can be numerically solved for s, u, v, ω. Note that the motion of B is independent of its mass density ρ.

2.1 Degenerate Case

The above derivation of differential equations (7), (8), (10), (13) is correct only if the denominators on their right hand sides do not vanish. Clearly (8) always holds following $|\alpha'|^2 > 0$. By parameterizing α and β as unit-speed curves with curvatures κ_α and κ_β, respectively, we can easily verify that the denominator in (7) vanishes only when one of the curves is concave at the contact with $\kappa_\alpha = \kappa_\beta$, a situation that almost never happens.

The vanishing of the denominator $\beta' \cdot \beta$ on the right in (10) implies that the contact force F passes through the center of mass of B, yielding zero torque. In the meantime, we have

$$\begin{aligned}
\beta' \cdot \beta \neq 0 \quad &\Rightarrow \quad \beta' \cdot \beta + \frac{\eta^2}{\beta' \cdot \beta}|\beta'|^2 \neq 0 \\
&\Rightarrow \quad \beta' \cdot (\beta + \frac{\eta^2}{\beta' \cdot \beta}\beta') \neq 0 \\
&\Rightarrow \quad R\beta' \cdot R(\beta + \frac{\eta^2}{\beta' \cdot \beta}\beta') \neq 0 \\
&\Rightarrow \quad \alpha' \cdot R(\beta + \frac{\eta^2}{\beta' \cdot \beta}\beta') \neq 0;
\end{aligned}$$

that is, the denominator in (13) does not vanish if $\beta' \cdot \beta \neq 0$.

Hence $\beta' \cdot \beta = 0$, or equivalently, $R\beta \times F = 0$, remains the only degenerate condition. It follows directly from (3) that

$$\dot{\omega} \quad = \quad -\frac{\mu g \int_B Rp \times \hat{v}_p \, dp}{\mathcal{A}\eta^2}. \tag{14}$$

Taking the dot products of $R\beta'$ with both sides of (2) we obtain

$$a \cdot R\beta' \quad = \quad -\frac{\mu g \int \hat{v}_p \, dp \cdot R\beta'}{\mathcal{A}}.$$

Taking the cross products of $R\beta'$ with both sides of (12) and substituting the above equation in, we have

$$\begin{aligned}
a \quad = \quad & -\Bigg(R\beta' \times \Big(\alpha'' \dot{u} \times (v_f - v) + \alpha' \times a_f \\
& - \Big(\alpha'' \dot{u} \cdot R\beta + \alpha' \cdot (\omega \times R\beta + R\beta' \dot{s}) \Big) \omega \Big) \\
& + (\alpha' \cdot R\beta)\dot{\omega} \times R\beta' + \frac{\mu g \int_B \hat{v}_p \, dp \cdot R\beta'}{\mathcal{A}} \alpha' \Bigg) \\
& \Big/ (\alpha' \cdot R\beta').
\end{aligned} \tag{15}$$

2.2 Integrals of Friction

To numerically integrate (7), (8), (10), and (13), it is necessary to evaluate the integral Γ that determines the role of friction on dynamics. Let us rewrite Γ as a linear sum of three subintegrals:

$$\begin{aligned}
\Gamma \quad = \quad & \int_B (R\beta' \cdot \hat{v}_p) Rp \, dp + (\beta' \cdot \beta) \int_B \hat{v}_p \, dp \\
& - \int_B (\beta' \cdot p) \hat{v}_p \, dp.
\end{aligned}$$

In the degenerate case, it is also required to evaluate the integral $\int_B Rp \times \hat{v}_p \, dp$ in equation (14).

When the object B is translating at velocity v, these evaluations are easy:

$$\begin{aligned}
\Gamma \quad &= \quad (\beta' \cdot \beta)\mathcal{A}\hat{v}; \\
\int_B Rp \times \hat{v}_p \, dp \quad &= \quad 0.
\end{aligned}$$

The case of the object translating at velocity $R^{-1}v = (v_x, v_y)$ and rotating about its center of mass at angular velocity $\omega \neq 0$ (all with respect to the body frame) can be regarded as the object rotating about some moving point $\omega \times (v_x, v_y)/\omega^2 = (-v_y/\omega, v_x/\omega)$, called the *instantaneous rotation center* (i.r.c.). In polar coordinates with respect to the i.r.c., all the aforementioned subintegrals are reducible to one-variable integrals [9].

For polygonal shapes, *closed* forms of Γ exist; for most other shapes, it can only be evaluated numerically.

2.3 Initial Accelerations

Given the initial contact positions $\alpha(u_0)$ on f and $\beta(s_0)$ on B, and the initial pose of f, the initial velocities are

$$v(0) = v_0 = 0, \quad \omega(0) = \omega_0 = 0, \quad \text{and} \quad v_f(0) = 0.$$

Plugging the above into (7) and (8) yields zero initial velocities of the contact point:

$$\dot{s}(0) = 0 \quad \text{and} \quad \dot{u}(0) = 0.$$

In the degenerate case where the contact normal N passes through the center of mass O, the initial acceleration and angular acceleration follow easily from (14) and (15):

$$\begin{aligned}
\dot{\omega}_0 \quad &= \quad -\frac{\mu g \int_B p \times N \, dp}{\mathcal{A}\eta^2} \\
&= \quad -\frac{\mu g \int_B p \, dp \times N}{\mathcal{A}\eta^2} \\
&= \quad 0; \\
a_0 \quad &= \quad -\frac{R\beta' \times (\alpha' \times a_f) + \mu g (N \cdot \beta')\alpha'}{\alpha' \cdot R\beta'} \\
&= \quad a_f - \frac{a_f \cdot R\beta'}{\alpha' \cdot R\beta'}\alpha'.
\end{aligned}$$

Here we write $\dot{v}(0) = a_0$ and $\dot{\omega}(0) = \dot{\omega}_0$.

In the non-degenerate case, we have $\dot{\omega}_0 \neq 0$. Under Coulomb's law, the frictional force f_p at $p \in B$ is opposed to the acceleration

$$\begin{aligned} a_p(0) &= \dot{v}_p(0) = a_0 + \dot{\omega}_0 \times p + \omega_0 \times (\omega_0 \times p) \\ &= a_0 + \dot{\omega}_0 \times p \\ &= \dot{\omega}_0(\frac{a_0}{\dot{\omega}_0} + 1 \times p). \end{aligned}$$

By a simple argument, the sign of $\dot{\omega}_0$ must agree with its sign were there no friction; hence it is known. Consequently, $\hat{a}_p(0), f_p$, and

$$\Gamma_0 = \int_B \Big(R\beta' \cdot \hat{a}_p(0)\Big)Rp + \Big(\beta' \cdot (\beta - p)\Big)\hat{a}_p(0)\, dp$$

become functions of $\frac{a_0}{\dot{\omega}_0}$. Thus (10) can be rewritten as

$$a_0 = \frac{\mathcal{A}\eta^2\dot{\omega}_0 \times R\beta' - \mu g \Gamma_0(\frac{a_0}{\dot{\omega}_0})}{\mathcal{A}\beta' \cdot \beta}. \quad (16)$$

Meanwhile, it follows from (12) that

$$\begin{aligned} \dot{\omega}_0 &= \frac{\alpha' \times (a_f - a_0)}{\alpha' \cdot R\beta} \\ &= \frac{\alpha' \times a_f}{\alpha' \cdot R\beta + \alpha \times \frac{a_0}{\dot{\omega}_0}}. \end{aligned} \quad (17)$$

Dividing both sides of (16) by $\dot{\omega}_0$ and substituting (17) in, we get the following equation in $\frac{a_0}{\dot{\omega}_0}$:

$$\frac{a_0}{\dot{\omega}_0} = \frac{\mathcal{A}\eta^2 \times R\beta' - \mu g \Gamma_0(\frac{a_0}{\dot{\omega}_0})\frac{\alpha' \cdot R\beta + \alpha \times \frac{a_0}{\dot{\omega}_0}}{\alpha' \times a_f}}{\mathcal{A}\beta' \cdot \beta}. \quad (18)$$

Equation (18) is solvable for $\frac{a_0}{\dot{\omega}_0}$ by the Newton-Raphson method, with the derivative $\partial\Gamma_0/\partial\frac{a_0}{\dot{\omega}_0}$ approximated by numerical differences. Hence a_0 and $\dot{\omega}_0$ are determined.

2.4 Contact Breaking

The only constraint that was left out in the derivation of differential equations (7), (8), (10), and (13) is inequality (5). This constraint, however, is used to check when the contact between the finger and the object breaks. More specifically, the contact breaks when $R\beta' \times F \leq 0$.

3 Sensing Initial Pose

Assume the presence of a tactile sensor attached to finger f that measures the value of parameter u at the contact on the finger boundary α. In addition, the initial pose of f is assumed to be known, and the controller is assumed to be exact so the finger velocity v_f is known. Thus, the initial pose of object B is completely characterized by parameter s_0 that gives the initial contact on object boundary β, and so is the contact motion u on α according to equations (7), (8), (10), and (13). Without any ambiguity, we denote the contact point on α at time t, with respect to initial pose s_0 of B, as $u(s_0, t)$.

Let finger f push object B for some time Δt. The sensing problem: Given contact positions $u_0, \ldots, u_{n-1}$ on f at time $t_0 = 0, t_1, \ldots, t_{n-1} = \Delta t$, respectively, during the pushing, find an initial pose(s) s_0 of B such that $u(s_0, t_i) = u_i$, for $0 \leq i \leq n-1$.

Let us look at two sensor values u_0 and u_1 first. Consider parameter u as a mapping, defined by the finger motion, from an initial pose s_0 of B to the contact position $u(s_0, t_1)$ on f at time t_1 subject to $u(s_0, 0) = u_0$. Since there exists no closed form of u, we can only solve the equation $u(s_0, t_1) = u_1$ numerically. For instance, the Newton-Raphson method can be used with numerical derivative $\frac{\partial u(s_0, t_1)}{\partial s_0}$.

Newton-Raphson may find multiple solutions to $u(s_0, t_1) = u_1$ with different initial guesses of s_0. This means that multiple initial poses of B may result in the same contact position on f at time t_1, which often turned out to be the case in our simulations to be discussed below. We need to verify these poses against sensor values $u_2, \ldots, u_{n-1}$ to eliminate the ambiguities.

4 Simulations and Experiments

Simulations were conducted on two types of fingers (lines and ellipses) and two types of objects (ellipses and polygons). All data were generated randomly.[3] We simulated three types of pushing: ellipse(finger)-ellipse(object), line-ellipse, and ellipse-polygon.

Closed forms of integral Γ exist for polygons but not for ellipses. On a Sparcstation 20, one evaluation of Γ takes about 0.15s for a hexagon and about 2s for an ellipse. The computation of initial accelerations as in Section 2.3 takes about 1.6s and 25s for these two shapes, respectively.

A push was performed for a certain amount of time (measured in the steps of forward integration on (7), (8), (10), and (13)). During the push, the initial, the final, and one intermediate contact positions on the finger were timed and recorded. The algorithm in Section 3 computed possible initial poses of the object which, under the push, would cause the contact to move from the initial position to the intermediate position on the finger at the recorded time. [4] The

[3] Random polygons were generated by taking random walks on an arrangement of a large number of random lines precomputed by a topological sweeping algorithm [5].

[4] More specifically, the algorithm guessed a number of initial contacts on the object, and called the Newton-Raphson routine. In the experiments, 10 guesses were taken for an ellipse and 3 guesses for each edge of a polygon.

final contact position was then used to distinguish between ambiguous poses.

Table 1 shows the sensing results under no friction between the object and the plane.[5] It suggests that the pose

type	# tests	# succs	succ ratio	time/test (min.)
ellips-ellips	1000	978	97.8%	1.11
line-ellips	1000	975	97.5%	1.51
ellips-poly	200	189	94.5%	5.06

Table 1: Sensing results in the frictionless plane.

of an object is often computable from three instantaneous contacts on a pushing finger.

The simulation outcome that the finger contacts u_0, u_1, u_2 at time instants t_0, t_1, t_2, respectively, often determine the object pose can be explained intuitively through Figure 3. Consider the mapping defined by the pushing from the initial object pose s_0 to the contact motion $u(s_0, t)$ on the finger, subject to $u(s_0, t) = u_0$. At time t_1, very likely multiple contact motions starting at u_0 will reach u_1, the intermediate contact position. This was observed in the simulations. But almost definitely, only one of these motions will also reach u_2 at time t_2.

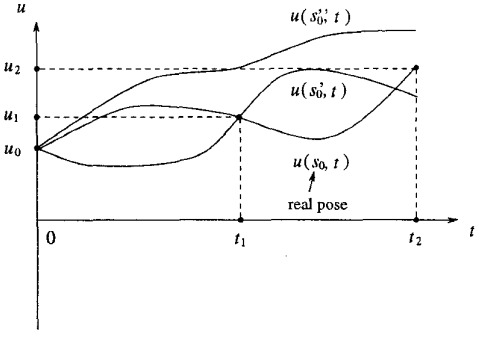

Figure 3: Explanation of how sensing works.

The slow numerical evaluation of integral Γ prohibits us from conducting large number of tests on sensing ellipses by pushing under sliding friction. Simulations under friction were only performed on polygons, for which closed forms of Γ exist. The 105 tests took about 65 hours, yielding 94 successes, 11 failures and ambiguities.

Later we conducted some experiments with an Adept 550 robot. The "finger" in our experiments was a plastic disc held by the robot gripper. Since no tactile sensor had been implemented, the disk edge was marked with angles from the disk center so a contact position could be read by flesh eyes. Plastic polygonal parts of different material were used as objects. A plywood surface served as the supporting plane for pushing. Figure 4 shows an experimental setup.

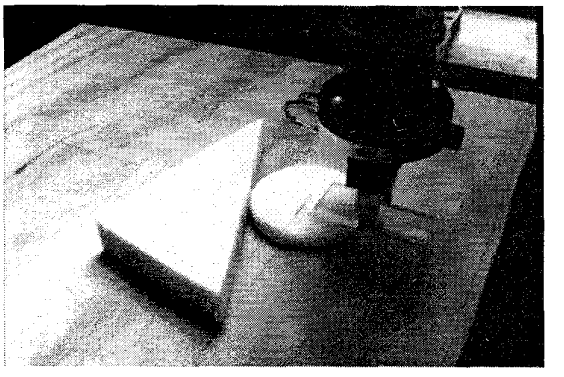

Figure 4: Experimental setup of pose-from-pushing. The coefficient of contact friction between the part and the disk (finger) was small (measured to be 0.213).

Simulation and experiment results on pushing were found to agree closely (Figure 5), with slight discrepancies

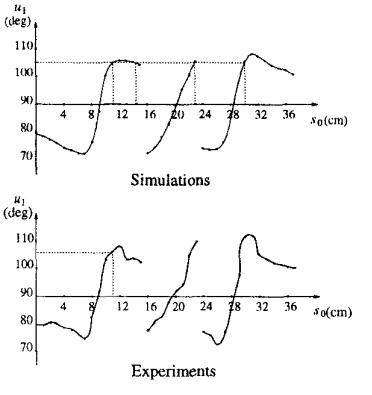

Figure 5: Simulations versus experiments on a triangular part. The initial contacts s_0 were chosen to be at discretized locations on the part boundary. The initial contact u_0 on the pushing disk was always at 90 degrees from its center. The same disk motion was used in all experiments. The dotted lines illustrate the case where s_0 = 11 (cm): Four feasible poses were found by the simulator from contact position u_1 after the push.

mainly due to shape uncertainties and non-uniform properties of the disk, the parts, and the plywood, all handmade.

We also did some experiments on sensing. Instead of one push, two consecutive pushes were performed so that the contact position after the first push served as the intermediate contact position.

[5]For the ease of testing large groups of data, only constant finger accelerations a_f were used in our simulations. However, the subsequent observations are expected to also hold for arbitrary a_f.

5 Summary

We have introduced a sensing method applicable to many grasping tasks. The method finds the pose of a known planar object by pushing it with a fingertip and "feeling" the contact motion. Pushing is viewed as a mapping from the one-dimensional set of possible initial poses [6] of the object to the set of contact motions on the fingertip; and sensing is viewed as its *inverse* mapping. Given an initial contact on the fingertip, the set of possible contact positions at any time instant during a push is one-dimensional and generally continuous. Conversely, only a finite number of initial object poses generally may result in a sensed contact position at that time instant. The real pose is further determined by sensing yet a third contact position.

Contact motions are derived from a set of differential equations that consist of the geometric and kinematic constraints, as well as the dynamics of pushing. A numerical algorithm is presented to find the initial pose of an object given a finite number of intermediate contact positions on a pushing finger. Although in some worst cases [9] sensing ambiguities cannot be eliminated even if the entire contact motion on the finger is known, simulation results demonstrate that the initial, the final, and one intermediate contact positions often suffice for determining the pose. A sensing failure may be recovered by repeated pushing at different portions of the object boundary.

This work is the first step of our ongoing research on grasping parts of known shapes and on the integration of sensing and grasping.

More work is needed on improving the efficiency of the sensing algorithm which is currently inadequate for any real applications where friction exists. For each part, we could discretize its boundary and precompile a table from which poses can be directly looked up with contact positions. We would like to extend the contact motion analysis to frictional pushing contacts. Other future work includes an extension to non-uniform pressure distributions, as well as the implementation of a tactile sensor capable of sensing timed contact positions.

Acknowledgements Thanks to Matt Mason for an interesting discussion on the topics of pushing and pressure distribution; and to Kevin Lynch for an introduction to his related work on active sensing by pushing using tactile feedback and for many helpful comments on the paper. Also thanks to the anonymous reviewers for their thorough reading and valuable comments.

[6] The initial contact on the fingertip can be sensed, and the fingertip normal is opposite to the object normal at the contact, as given by equation (6).

References

[1] Srinivas Akella and Matthew T. Mason. Posing polygonal objects in the plane by pushing. In *Proceedings of the 1992 IEEE International Conference on Robotics and Automation*, pages 2255–2262, 1992.

[2] J. C. Alexander and J. H. Maddocks. Bounds on the friction-dominated motion of a pushed object. *International Journal of Robotics Research*, 12(3):231–248, 1993.

[3] Chunsheng Cai and Bernard Roth. On the spatial motion of a rigid body with point contact. In *Proceedings of the 1987 IEEE International Conference on Robotics and Automation*, pages 686–695, 1987.

[4] Bruce R. Donald, James Jennings, and Daniela Rus. Analyzing teams of cooperating mobile robots. In *Proceedings of the 1994 IEEE International Conference on Robotics and Automation*, pages 1896–1903, 1994.

[5] Herbert Edelsbrunner and Leonidas J. Guibas. Topologically sweeping an arrangement. In *Proceedings of the 18th Annual ACM Symposium on Theory of Computing*, pages 389–403. ACM Press, 1986. Berkeley, CA.

[6] Suresh Goyal, Andy Ruina, and Jim Papadopoulos. Planar sliding with dry friction. *Wear*, 143:307–352, 1991.

[7] Robert D. Howe and Mark R. Cutkosky. Touch sensing for robotic manipulation and recognition. In *The Robotics Review 2*, pages 55–112. The MIT Press, Cambridge, 1992.

[8] Yan-Bin Jia and Michael Erdmann. Geometric sensing of known planar shapes. *International Journal of Robotics Research*, 15(3), 1996.

[9] Yan-Bin Jia and Michael Erdmann. Pose from pushing. Technical Report CMU-RI-96-??, CMU Robotics Institute, 1996. To appear.

[10] Zexiang Li and John Canny. Motion of two rigid bodies with rolling constraint. *IEEE Transactions on Robotics and Automation*, 6(1):62–72, 1990.

[11] Kevin Lynch, Hitoshi Maekawa, and Kazuo Tanie. Manipulation and active sensing by pushing using tactile feedback. In *Proceedings of the 1992 IEEE/RSJ International Conference on Intelligent Robots and Systems*, pages 416–421, 1992.

[12] William Duncan MacMillan. *Dynamics of Rigid Bodies*. Dover Publications, Inc., 1936.

[13] Matthew T. Mason. Mechanics and planning of manipulator pushing operations. *International Journal of Robotics Research*, 5(3):53–71, 1986.

[14] David J. Montana. The kinematics of contact and grasp. *International Journal of Robotics Research*, 7(3):17–32, 1988.

[15] Jong-Shi Pang and Jeffrey C. Trinkle. Complementary formulations and existence of solutions of dynamic multi-rigid-body contact problems with Coulomb friction. *Journal of Mathematical Programming*, 1996. To appear.

[16] M. Spivak. *A Comprehensive Introduction to Differential Geometry*. Publish or Perish Inc., 1975.